77721

P - 23

Comparison of Jet Plume Shape Predictions and Plume Influence on Sonic Boom Signature

Raymond L. Barger
and N. Duane Melson

NASA

Comparison of Jet Plume Shape Predictions and Plume Influence on Sonic Boom Signature

Raymond L. Barger
and N. Duane Melson
Langley Research Center
Hampton, Virginia

Abstract

An Euler shock-fitting marching code yields good agreement with semiempirically determined plume shapes, although the agreement decreases somewhat with increasing nozzle angle and the attendant increase in the nonisentropic nature of the flow. Some calculations for a low-boom configuration with a sample engine indicated that, for flight at altitudes above 60 000 ft, the plume effect is dominant. This negates the advantages of a low-boom design. At lower altitudes, plume effects are significant but of the order that can be incorporated into the low-boom design process.

Introduction

The plume that results from an underexpanded jet is a significant factor in assessing the feasibility of potential supersonic commercial aircraft because of its influence on the sonic boom signature and on aerodynamic performance. Consequently, reliable procedures for computing both the plume shape and the effects of the plume on the sonic boom signature are required. This report presents a comparison of plume shapes computed by several methods, together with an examination of the kinds of sonic boom effects the plume introduces.

The primary reference in the current literature on plume shapes and plume sonic boom effects is reference 1. This reference describes a combined experimental-computational study to determine empirically the shapes of jet equivalent solid bodies, that is, an effective discrete jet free-stream slip line. These shapes were compared with plume shapes predicted by two computational methods. Reference 1 also includes some sample calculations to illustrate the plume sonic boom effect.

The present report describes calculations that yield a closer correlation with the semiempirically determined shapes than the methods described in reference 1. Also included is a study of the influence of flight altitude and configuration geometry on the problem of plume sonic boom effects with some illustrative examples.

Symbols

$A(x)$	equivalent area distribution
D	external nozzle exit diameter, d + Lip thickness
d	internal nozzle diameter at jet exit, $2h$
F	value of Whitham F-function
h	internal nozzle radius at jet exit

L	airplane reference length
M	Mach number
p	static pressure
Δp	$= p - p_o$
r	radial coordinate
t	time
$t = 0$	time at which a pulse, traveling at ambient sound speed, arrives at ground
x	coordinate in direction of nozzle axis
α	nozzle expansion angle
β	nozzle boattail angle
ϵ	dummy integration variable

Subscripts:

j	jet
o	undisturbed condition
∞	free stream

Plume Calculations

The plume shapes were computed with the Euler shock-fitting marching code described in reference 2. Calculations were made for some, but not all, of the nozzle shapes and conditions included in the investigation described in reference 1. Calculations were not made for the boattailed shapes because the plume code could not treat this case without modification.

The type of nozzle that was tested is depicted in figure 1. The nozzle divergence angles α for the non-boattailed shapes were 7.28°, 9.06°, and 11.50°. The measurements of reference 1 indicated that, for the two larger divergence angles, an internal shock was generated inside the nozzle. This shock is apparently associated with the curvature discontinuity that occurs where the circular-arc throat section meets the conical nozzle section. The experimental results indicated that this shock was relatively weak and its

presence was not considered in the direct calculation of the plume shape or in the calculation of the exit Mach number.

Figure 2 shows a set of calculations for plumes emitted from the nozzle with $\alpha = 11.5°$. In this figure, the solid line indicates the semiempirically determined jet equivalent plume shape. It was obtained by measuring the flow conditions along a line outside the plume and parallel to the nozzle axis. Then, with these initial conditions, a characteristic net was computed inward, taking the streamline that matches the nozzle lip as the jet equivalent solid body.

The dash lines in figure 2 denote calculations, reported in reference 1, by a linearized technique described in reference 3. The long-dash–short-dash lines, also from reference 1, denote calculations by a method of characteristics assuming straight shock lines and conical nozzle flow. The circles denote calculations by the Euler method of reference 2.

All these calculations predict plume shapes larger than the semiempirically determined shapes. The discrepancy is significantly smaller for the Euler calculation.

Figure 3 shows a similar comparison of computed and semiempirically determined shapes for a nozzle with $\alpha = 9.06°$. For this nozzle, the points calculated by the Euler method represent a close approximation to the empirical shape, although it is still slightly overpredicted.

The nozzle with $\alpha = 7.28°$ was tested at only one pressure ratio. For this case, shown in figure 4, the Euler method yields an excellent representation of the empirically determined shape.

Thus these results indicate that as the nozzle expansion angle increases, the correlation of the Euler calculations and the empirical results tends to deteriorate. As the nozzle angle increases, the observation was made that an internal shock forms. If this shock significantly reduces the Mach number at the nozzle lip, this effect would account for at least part of the disagreement, since the exit Mach number is computed in reference 1 with the assumption of isentropic nozzle flow. However, a number of other factors could be involved. These factors include viscous effects, the effect of the bluntness of the nozzle lip, and assumptions involved in initializing the Euler plume code. Some attempts were made to determine the precise nozzle exit flow by computing the internal nozzle flow field by time-relaxation Euler codes, but these attempts failed to yield the type of shock structure observed in the experimental results.

No further attempt was made to investigate the various sources of error. The accuracy of the computed shapes is probably consistent with the accuracy of the approximate procedures that are used to obtain the effective area distributions that are required for sonic boom calculations (ref. 4). For the purpose of comparing computed shapes with the semiempirical shapes of reference 1, a simple adjustment formula could be applied, since the discrepancy increases with nozzle divergence angle in a systematic manner.

Sonic Boom Considerations

Once the jet plumes have been modelled as equivalent solid bodies their sonic boom effects can readily be determined. The equivalent solid body is simply treated as an extension of the engine nacelle. Then an equivalent area distribution obtained from projected Mach slice cuts through the configuration is generated. This area distribution is added to an equivalent area distribution due to lift to obtain a total area distribution $A(x)$. This area distribution is related to the sonic boom wave shape through the "F-function" which is defined by the formula

$$F(x) = \frac{1}{2\pi} \int_0^x \frac{A''(x - \epsilon)\, d\epsilon}{\sqrt{x - \epsilon}}$$

The wave shape is determined directly from the F-function, and the ground level signature is determined by a propagation and shock-fitting code. These concepts are explained in greater detail in the standard sonic boom literature. (See, for example, ref. 5.)

In view of the wide variety of approaches to configuration geometry and aircraft cruise conditions that are being considered for civil supersonic aircraft, it would not be practical at this point to attempt to compute plume effects for each case. However, a few calculations in addition to those already reported in reference 1 may serve to indicate the types and orders of magnitude of the effects to be expected.

Some factors involved are the flight Mach number and altitude, the configuration geometry, and the manner in which the engine nacelles are integrated into the geometry. Configurations that are designed for diminished sonic boom levels are usually laid out in such a way that the lift is distributed longitudinally to the greatest possible extent. The result is a planform somewhat like that shown schematically in figure 5(a). This geometry may be compared with that of a conventional supersonic fighter-type design with a more concentrated lift distribution (fig. 5(b)) or with a conventional civil transport configuration

without highly distributed lift but with an extensively notched arrow wing (fig. 5(c)).

For a relatively high flight altitude, the ambient pressure is so low that the nozzle flow is greatly underexpanded and consequently large plume effects are realized. For example, figure 6 shows the plume shape computed for a high performance afterburning engine with assumed ambient pressure equivalent to that at 60 000 ft ($M_\infty = 3.0$, $p_j/p_\infty = 8.86$). Flow parameters for this engine were computed by the method of reference 6. The pluming is significant, and consequently, the plumes for the four engines would contribute a significant equivalent area. The actual effect on the F-function and ground level signature is shown in figure 7 for a low-boom configuration of the type shown in figure 5(a). Figure 7(a) represents the F-function and signature with a cylindrical afterbody (no pluming) assumed, and figure 7(b) shows the corresponding results with the plume of figure 6. The plume has a dominant effect on the sonic boom signature for this case. The compression associated with the plume causes a shock of such magnitude that it moves forward and overrides the nose shock. The ground level overpressure is increased from a level slightly under 1 psf (fig. 7(a)) to about 2.2 psf (fig. 7(b)). It would not be feasible to attempt to tailor the configuration to allow for the additional area associated with this plume, since this area is so large.

However, the problem is mitigated at lower altitudes where the ambient pressure is higher and the plume is consequently smaller. Figure 8 shows the plume shape (with the same engine) for flight at 55 000 ft and $M_\infty = 2.1$. This plume is considerably smaller than that shown in figure 6, but it still has a significant effect on the F-function and signature. Figure 9(a) gives these results for the configuration with no plume, and figure 9(b) gives the corresponding results with the plume effect included. In this case the plume compression significantly alters the F-function and the signature, but the effect is much smaller than in the previous case.

A cursory effort was made to reduce the plume effect further by staggering the engine nacelles a distance of 10 ft and making modest changes (about 20-percent local variation) in the fuselage area distribution. The result, shown in figure 10, is some reduction of the plume effect. The maximum overpressure is reduced from 1.8 to 1.6 psf. Further reduction could probably be realized through a more systematic design approach (ref. 7), which might incorporate techniques such as those of references 8 and 9.

Reducing the flight altitude from 65 000 to 55 000 ft is so effective in reducing the plume effect that it would appear that, by extrapolation, a further reduction in cruise altitude, say to 45 000 ft, would render the plume effect negligible. However, such an extrapolation cannot be made. The high performance afterburning engines are not appropriate for the lower altitude flight, which would be associated with a lower Mach number.

Consequently, a sample case was computed for $M = 1.6$ flight at $M_\infty = 1.6$ and 45 000 ft with conventional turbo engines having an internal nozzle expansion of about 58 percent. The results are shown in figures 11 and 12. Figure 11 shows the plume shape. Figure 12(a) shows the F-function and signature with the assumption of a cylindrical plume, and figure 12(b) gives the corresponding results with the plume shape of figure 11. Again, a slight reduction in the plume effect can be realized by staggering the engines and tailoring the fuselage (fig. 13). This tailoring is substantial, about a 40-percent variation in cross-sectional area, as is shown in figure 14.

The results given in figures 9 and 11 may be compared with some calculations shown in figure 20 of reference 1. Those calculations demonstrate that, for configurations like the ones depicted in figures 5(b) and 5(c), relatively small jet plumes actually have a favorable effect on the sonic boom signature. The explanation for this difference involves both the amplitude of the aft expansion region of the F-function and the location of the plume effect relative to this expansion region. Low-boom configurations have a relatively gradual, low amplitude expansion (as illustrated in figs. 7(a), 9(a), and 12(a)), which results in a ground level amplitude of about 1.0 to 1.5 psf. When the compressive effect of the plume is imposed on the expanding flow, it is only partially cancelled by the expansion and leaves a secondary compression. On the other hand, a conventional configuration design, like that of figure 5(b) or (c), has a more sudden and larger amplitude expansion region in the F-function; this leads to a ground level amplitude on the order of 2.5 psf (ref. 1). In this case, the plume compression can be completely submersed in this expansion.

Figure 5(b) also illustrates another means that can be effective in controlling the location of the plume. Engine nacelles mounted on the fuselage can be situated in the optimum longitudinal position.

It should be emphasized that the configurations of figures 5(b) and (c) are not low-boom designs. Even with some reduction of the tail wave strength, the concentrated lift distributions associated with such

designs generally yield unacceptably high compressive overpressures.

Concluding Remarks

An Euler shock-fitting marching code yielded relatively good agreement with semiempirically determined plume shapes, although the agreement decreased somewhat with increasing nozzle expansion angle. Some evidence indicates that the discrepancy may be attributable to nonisentropic internal nozzle flow which is not accounted for in initializing the plume calculation.

Some calculations were carried out to obtain a general assessment of the nature and orders of magnitudes of the plume effects on the sonic boom signature. The calculations were for a low-boom configuration with a high performance engine. The results indicated that, for flight at altitudes above 60 000 ft, the plume effects were dominant; but for altitudes below 55 000 ft, they were significant but not dominant.

Some factors associated with incorporating the plume shape into the configuration design were also discussed.

NASA Langley Research Center
Hampton, VA 23665-5225
January 24, 1992

References

1. Putnam, Lawrence E.; and Capone, Francis J.: *Experimental Determination of Equivalent Solid Bodies To Represent Jets Exhausting Into a Mach 2.20 External Stream.* NASA TN D-5553, 1969.

2. Salas, Manuel D.: The Numerical Calculation of Inviscid Plume Flow Fields. AIAA Paper No. 74-523, June 1974.

3. Englert, Gerald W.: *Operational Method of Determining Initial Contour of and Pressure Field About a Supersonic Jet.* NASA TN D-279, 1960.

4. Middleton, W. D.; Lundry, J. L.; and Coleman, R. G.: *A System for Aerodynamic Design and Analysis of Supersonic Aircraft. Part 2 User's Manual.* NASA CR-3352, 1980.

5. Hayes, Wallace D.; Haefeli, Rudolph C.; and Kulsrud, H. E.: *Sonic Boom Propagation in a Stratified Atmosphere, With Computer Program.* NASA CR-1299, 1969.

6. Geiselhart, Karl A.; Caddy, Michael J.; and Morris, Shelby J., Jr.: *Computer Program for Estimating Performance of Air-Breathing Aircraft Engines.* NASA TM-4254, 1991.

7. Darden, Christine M.: *Sonic-Boom Minimization With Nose-Bluntness Relaxation.* NASA TP-1348, 1979.

8. Barger, Raymond L.; and Adams, Mary S.: *Fuselage Design for a Specified Mach-Sliced Area Distribution.* NASA TP-2975, 1990.

9. Mack, Robert J.; and Needleman, Kathy E.: *A Semiempirical Method for Obtaining Fuselage Normal Areas From Fuselage Mach Sliced Areas.* NASA TM-4228, 1991.
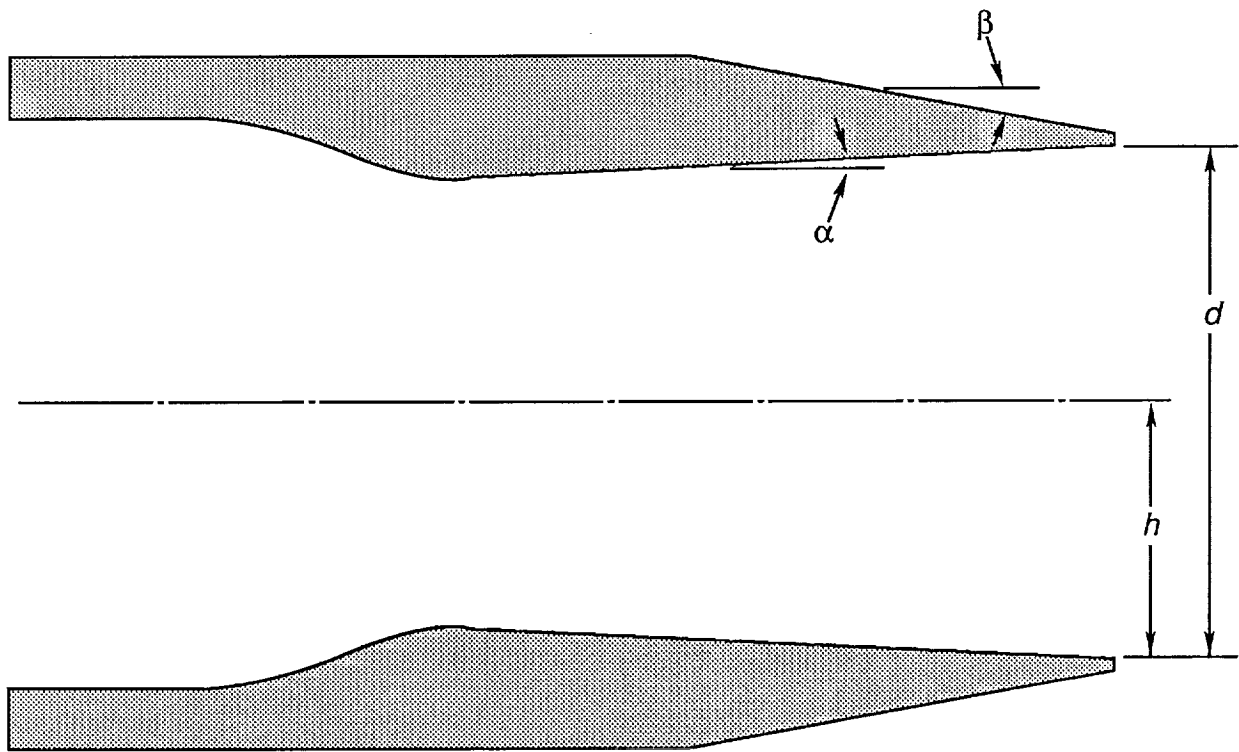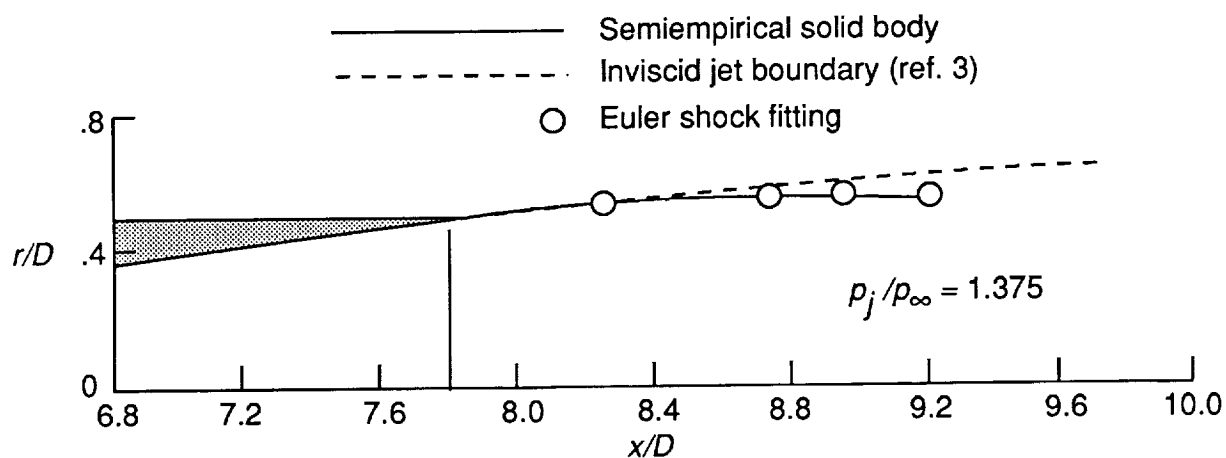
Figure 1. Nozzle geometry.
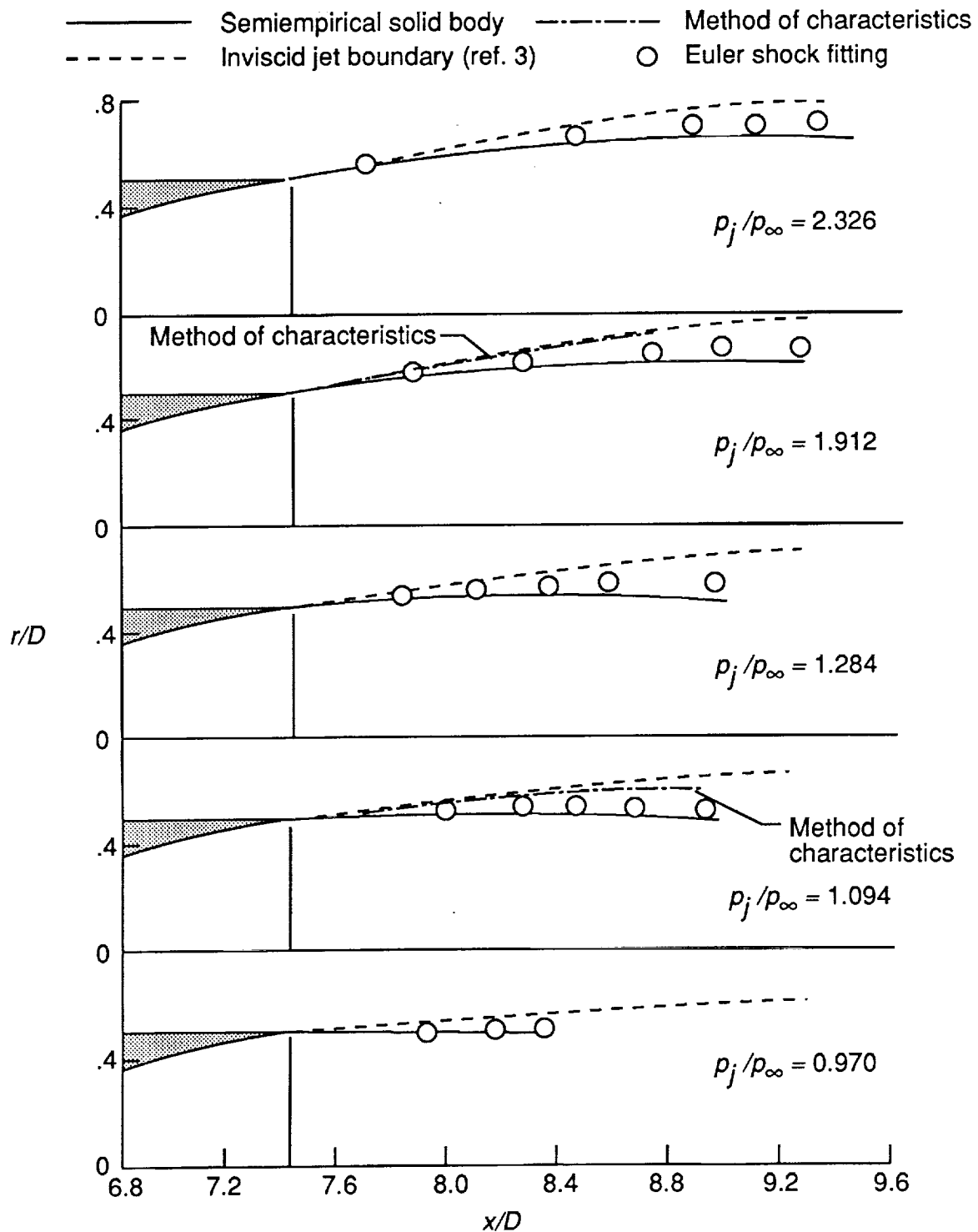
Figure 2. Semiempirical and computed plume shapes for nozzle with $\alpha = 11.50°$. $M_\infty = 2.2$; $M_j = 2.523$.
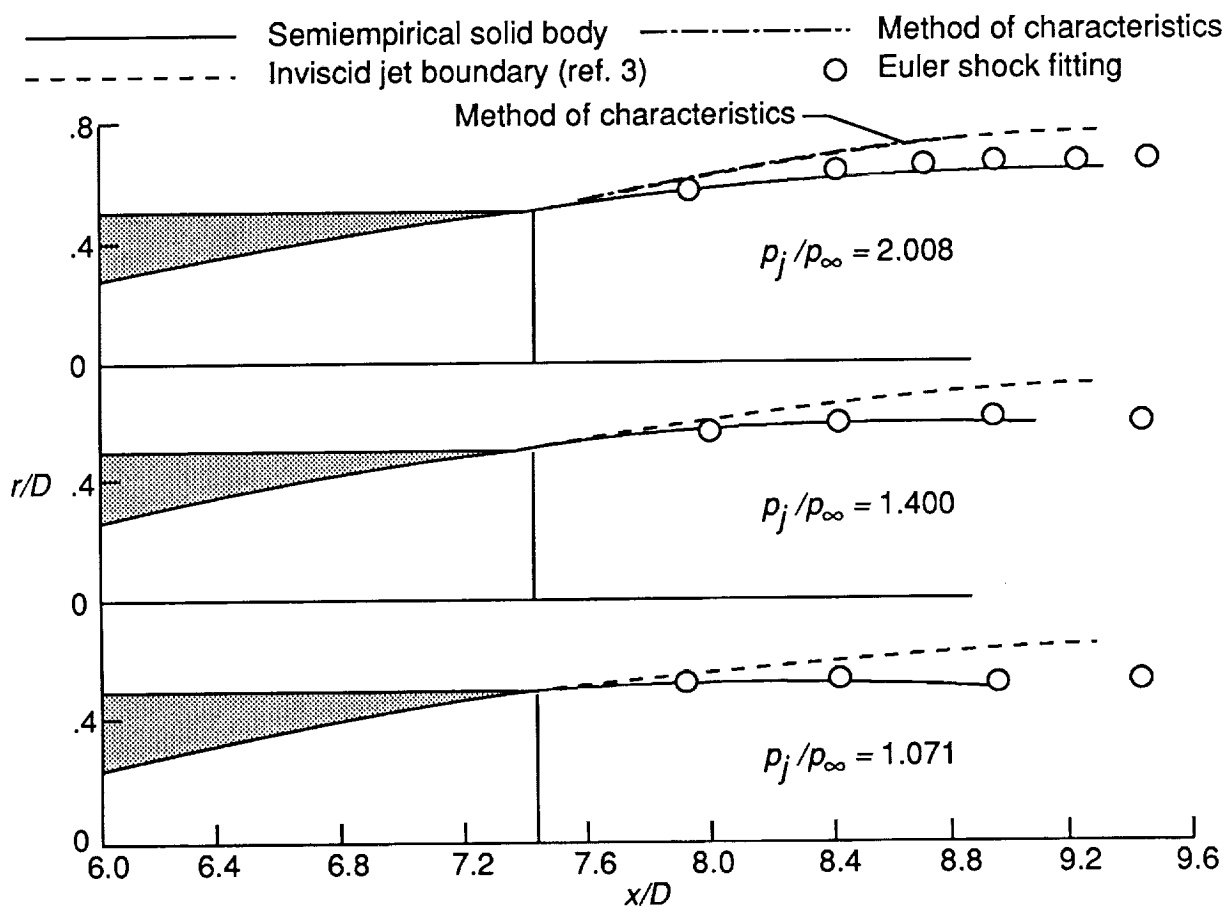
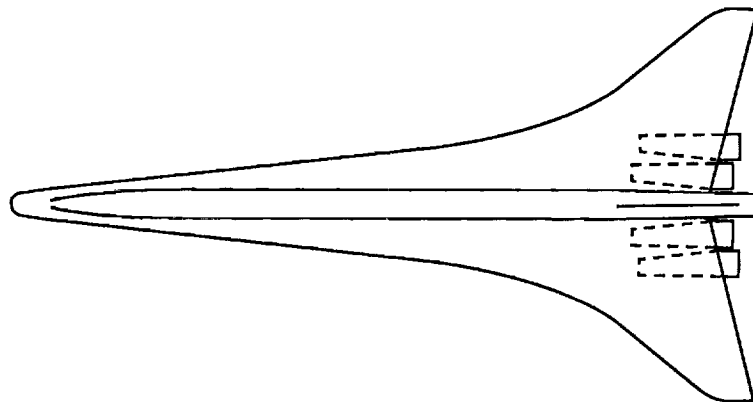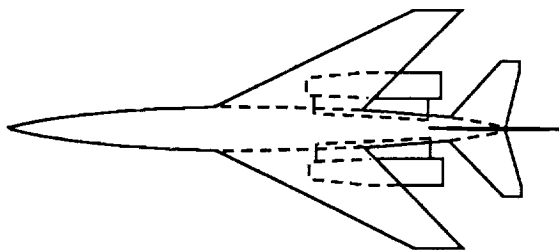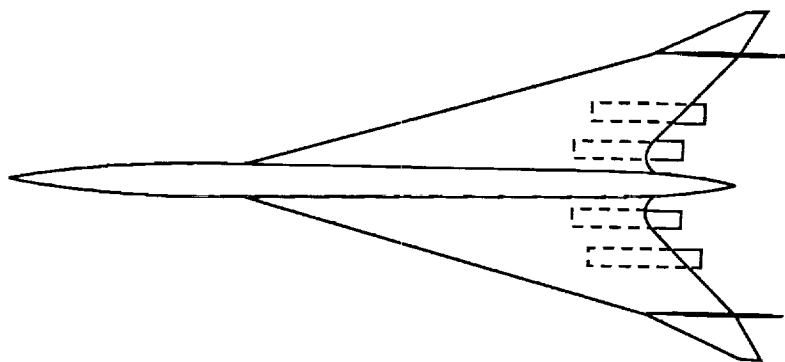Figure 3. Semiempirical and computed plume shapes for nozzle with $\alpha = 9.06°$. $M_\infty = 2.2$; $M_j = 2.267$.

Figure 4. Semiempirical and computed plume shapes for nozzle with $\alpha = 7.28°$. $M_\infty = 2.2$; $M_j = 2.272$.

(a) Low-boom design.

(b) Fighter configuration with nacelles mounted from fuselage.

(c) Commercial transport with notched wings.

Figure 5. Three types of supersonic configurations.
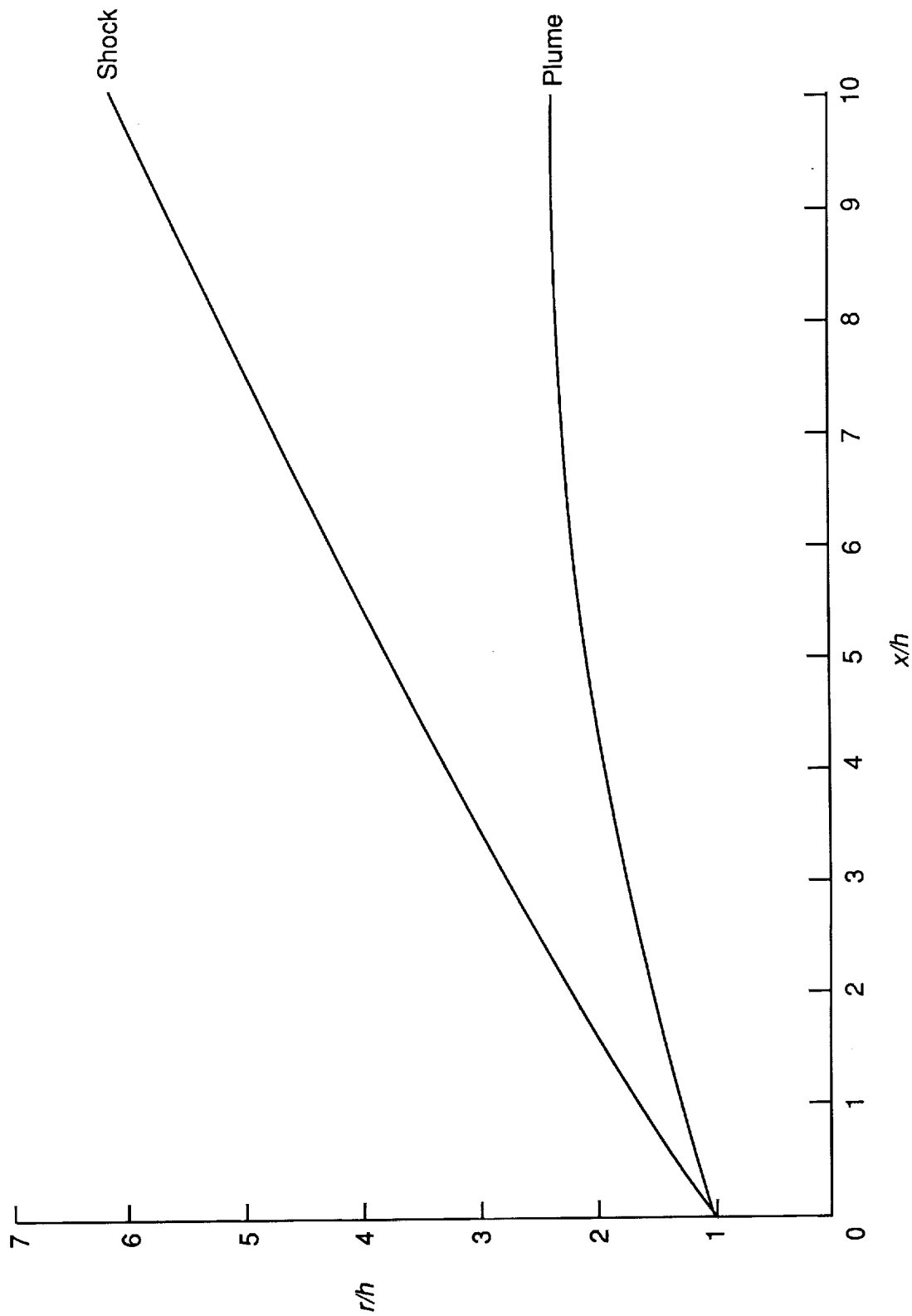
Figure 6. Computed plume shape for flight at $M_\infty = 3.0$ and altitude of 60 000 ft.
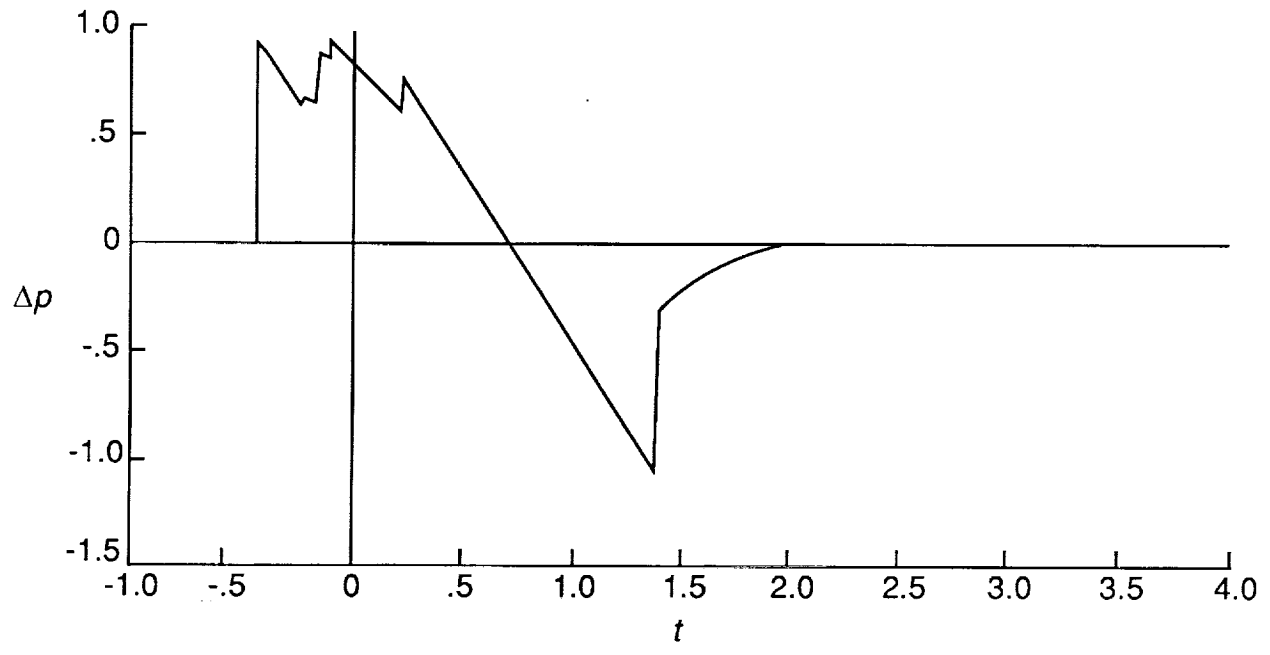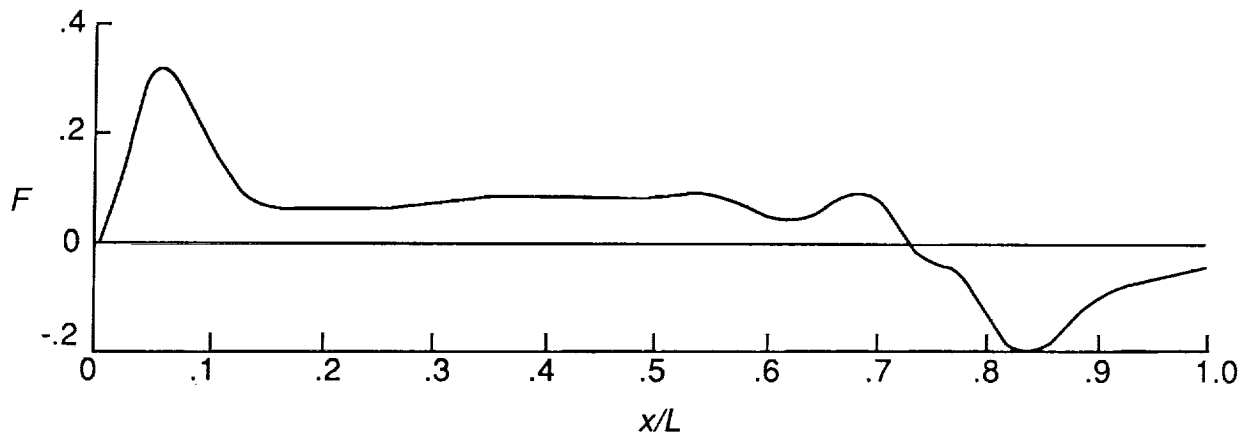
(a) Cylindrical jet.

Figure 7. F-functions and ground level signatures for low-boom configuration with cylindrical jet and computed plume of figure 6 at $M_\infty = 3.0$ and altitude of 60 000 ft.
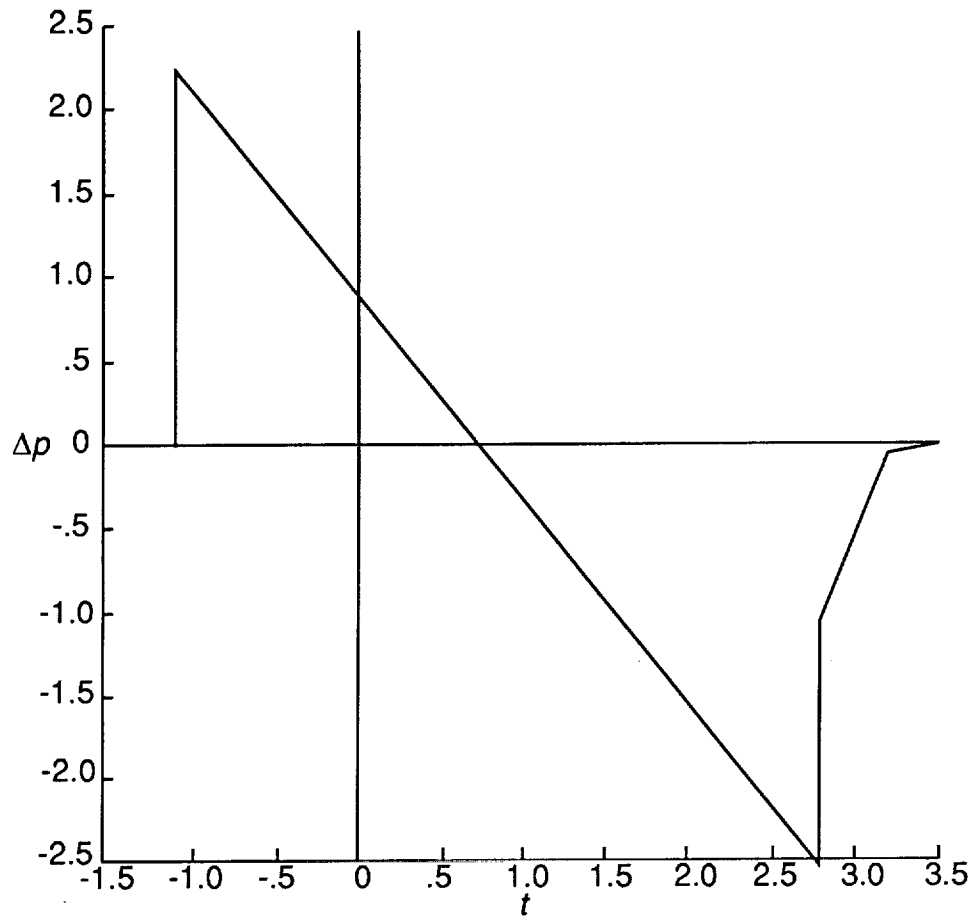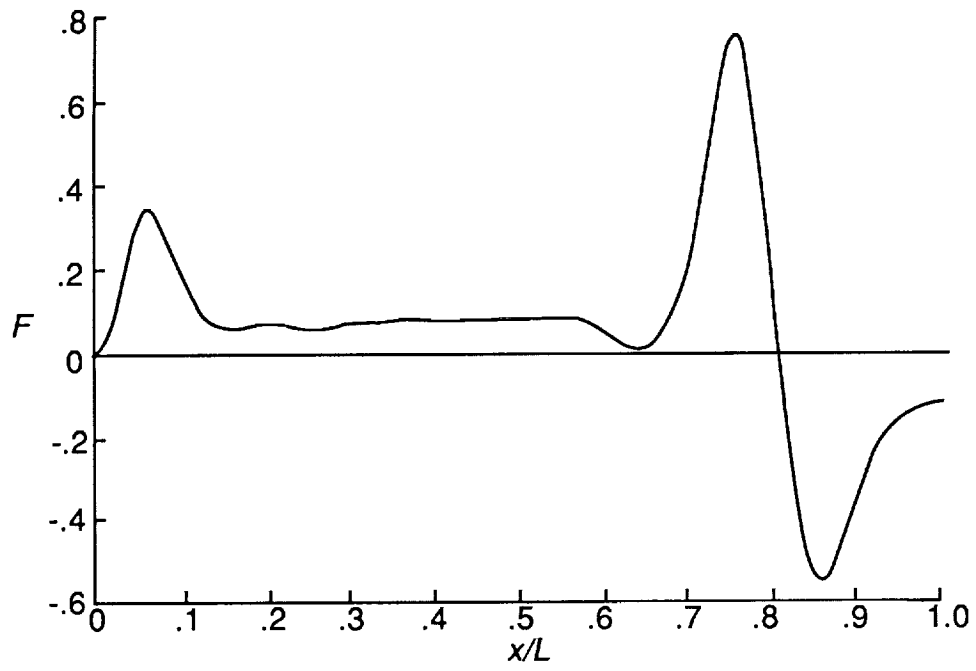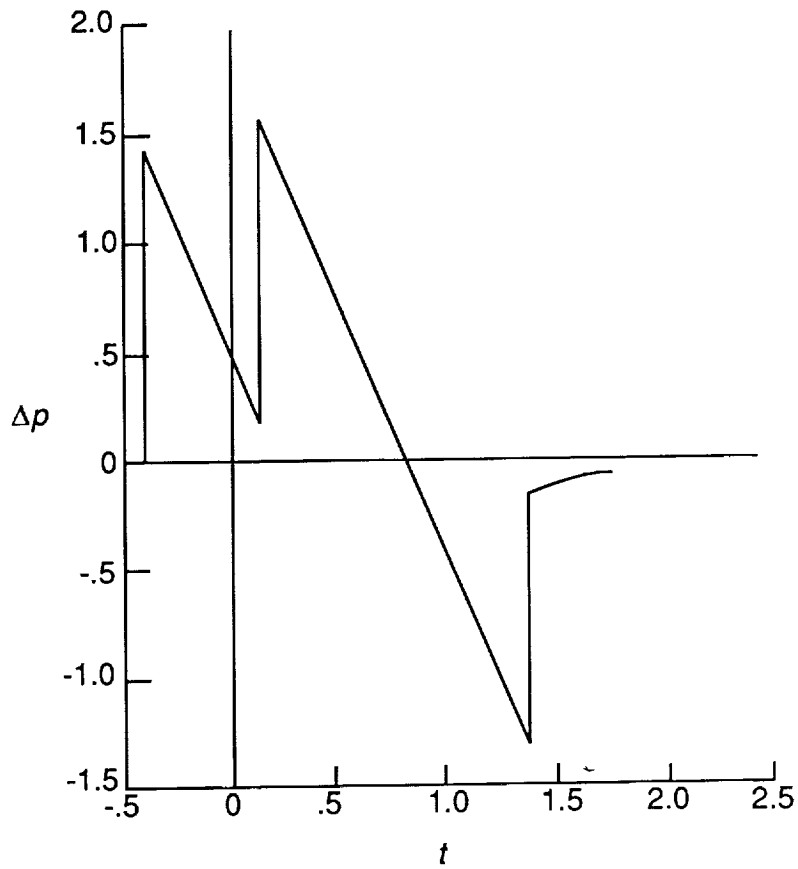
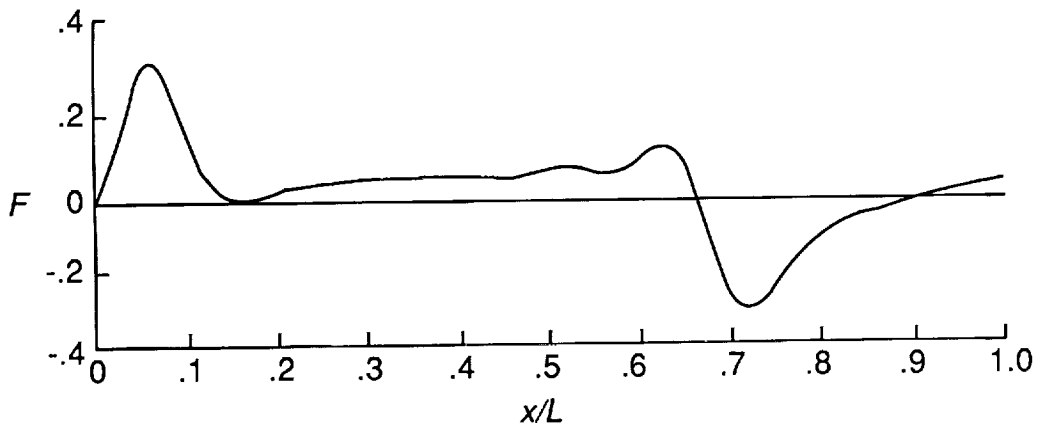(b) Computed plume of figure 6.

Figure 7. Concluded.
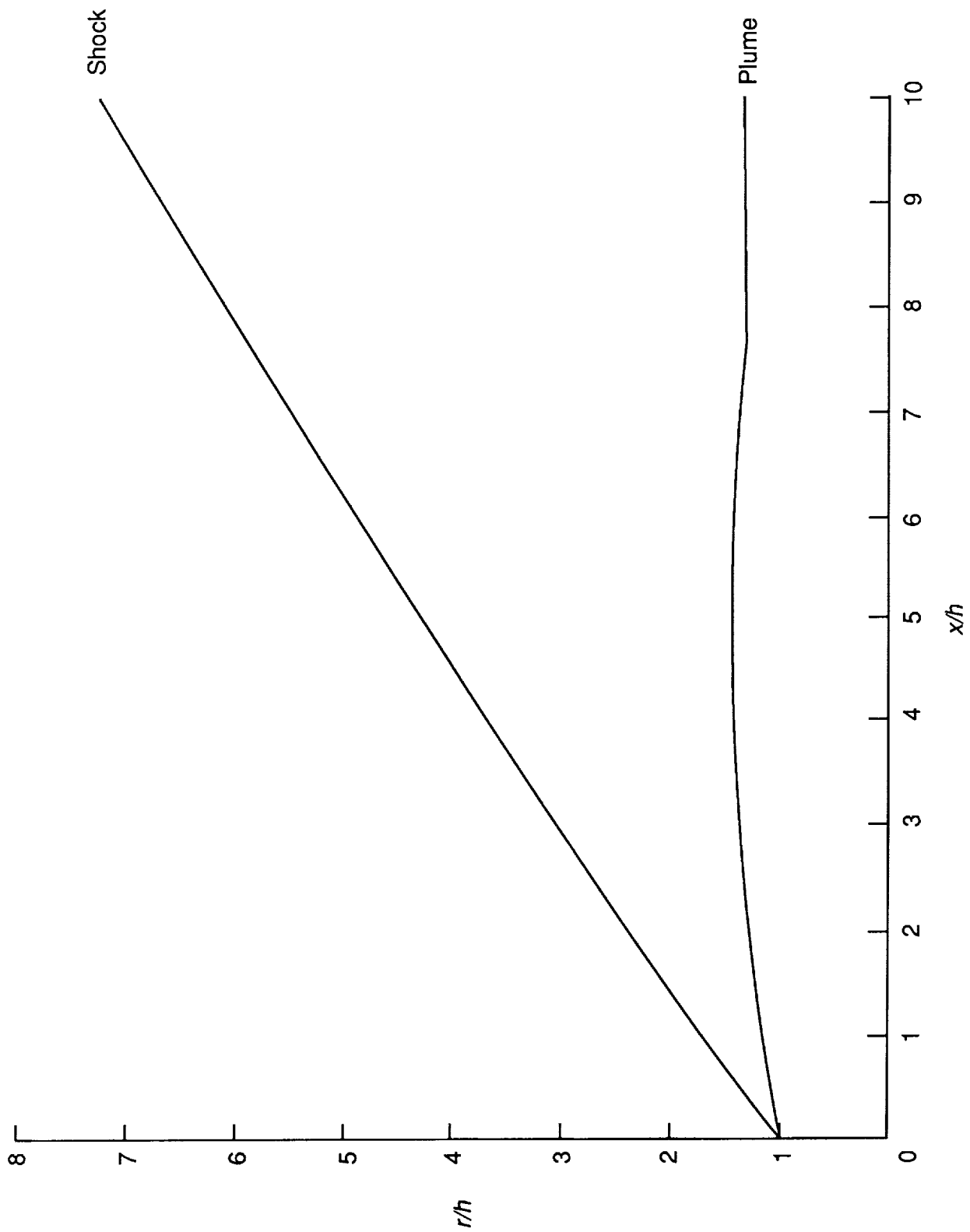
Figure 8. Computed plume shape for flight at $M_\infty = 2.1$ and altitude of 55 000 ft.
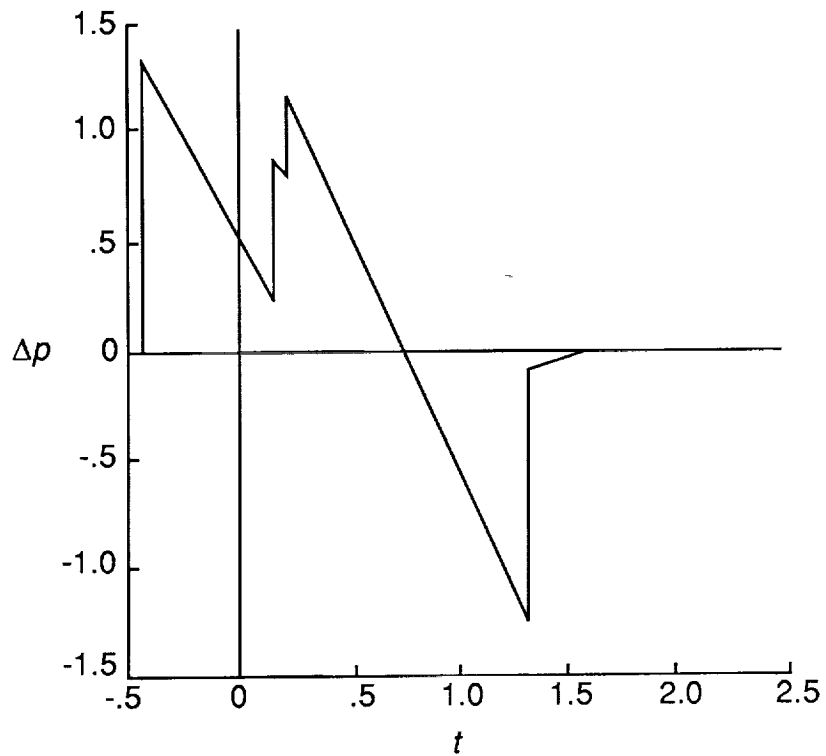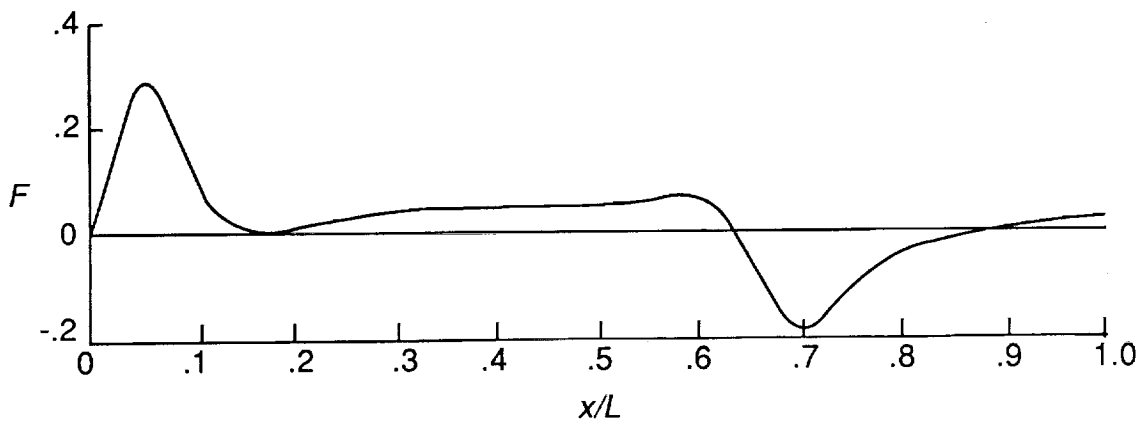
(a) Cylindrical jet.

Figure 9. F-functions and ground level signatures for low-boom configuration with cylindrical jet and computed plume of figure 6 at $M_\infty = 2.1$ and altitude of 55 000 ft.
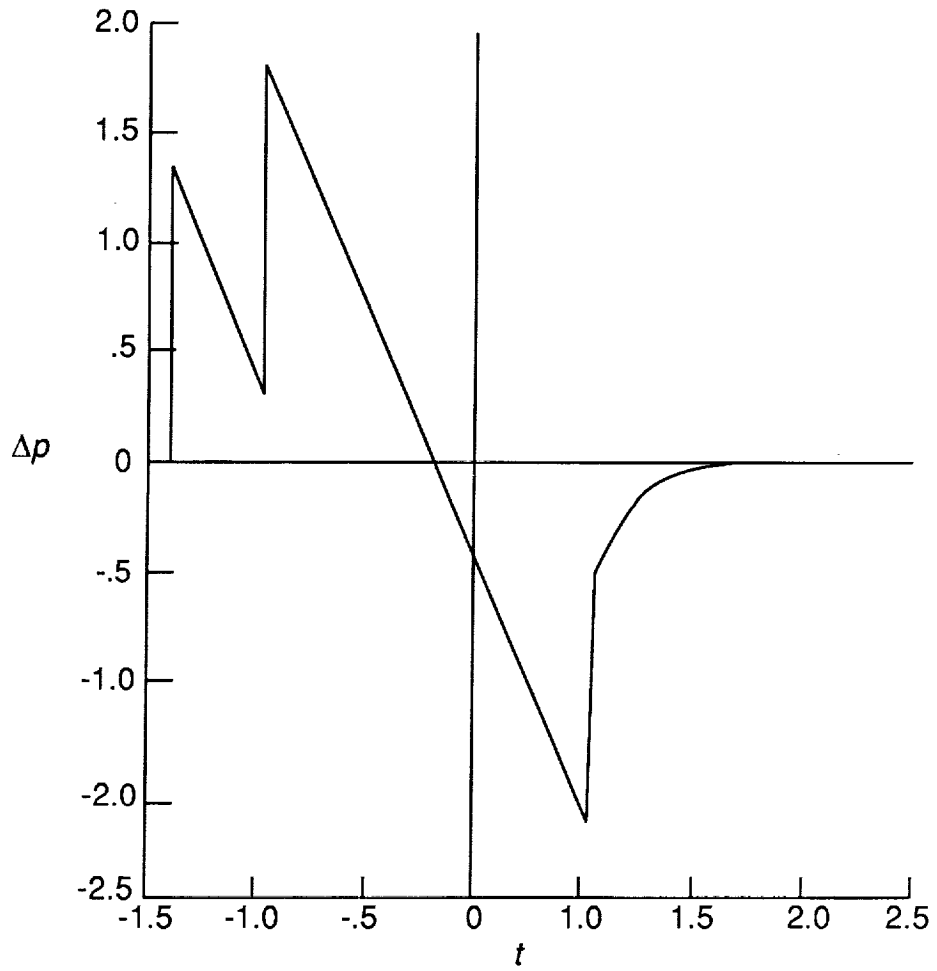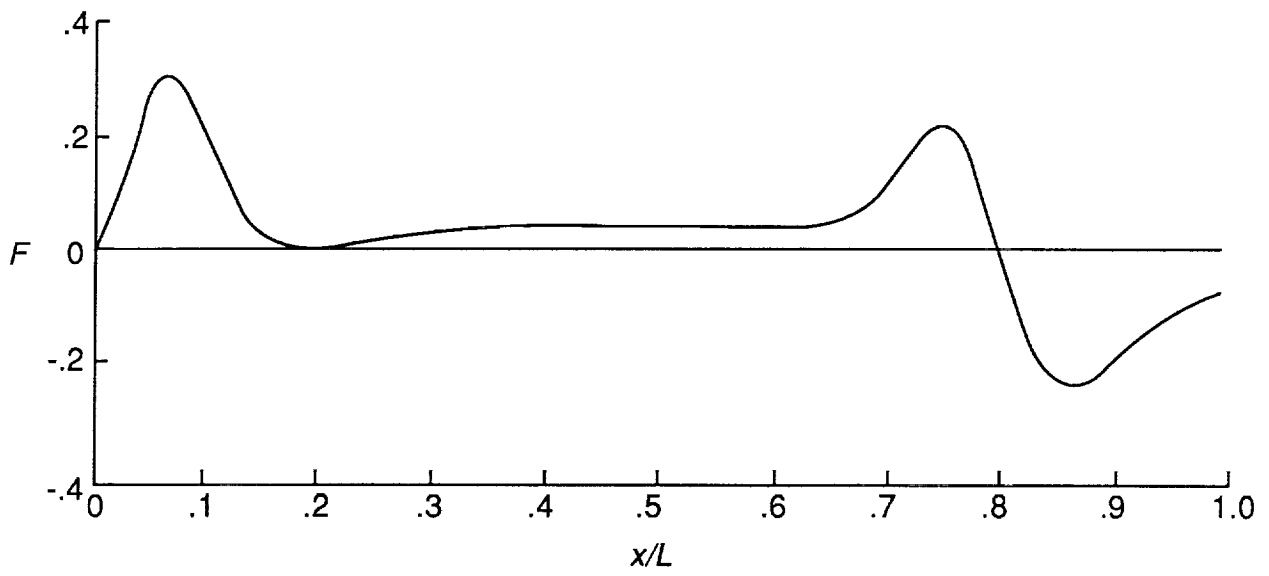
(b) Computed plume of figure 6.

Figure 9. Concluded.

Figure 10. F-function and ground level signature for low-boom configuration with the computed plume of figure 6 at $M_\infty = 2.1$ and altitude of 55 000 ft with modified fuselage and staggered engines.
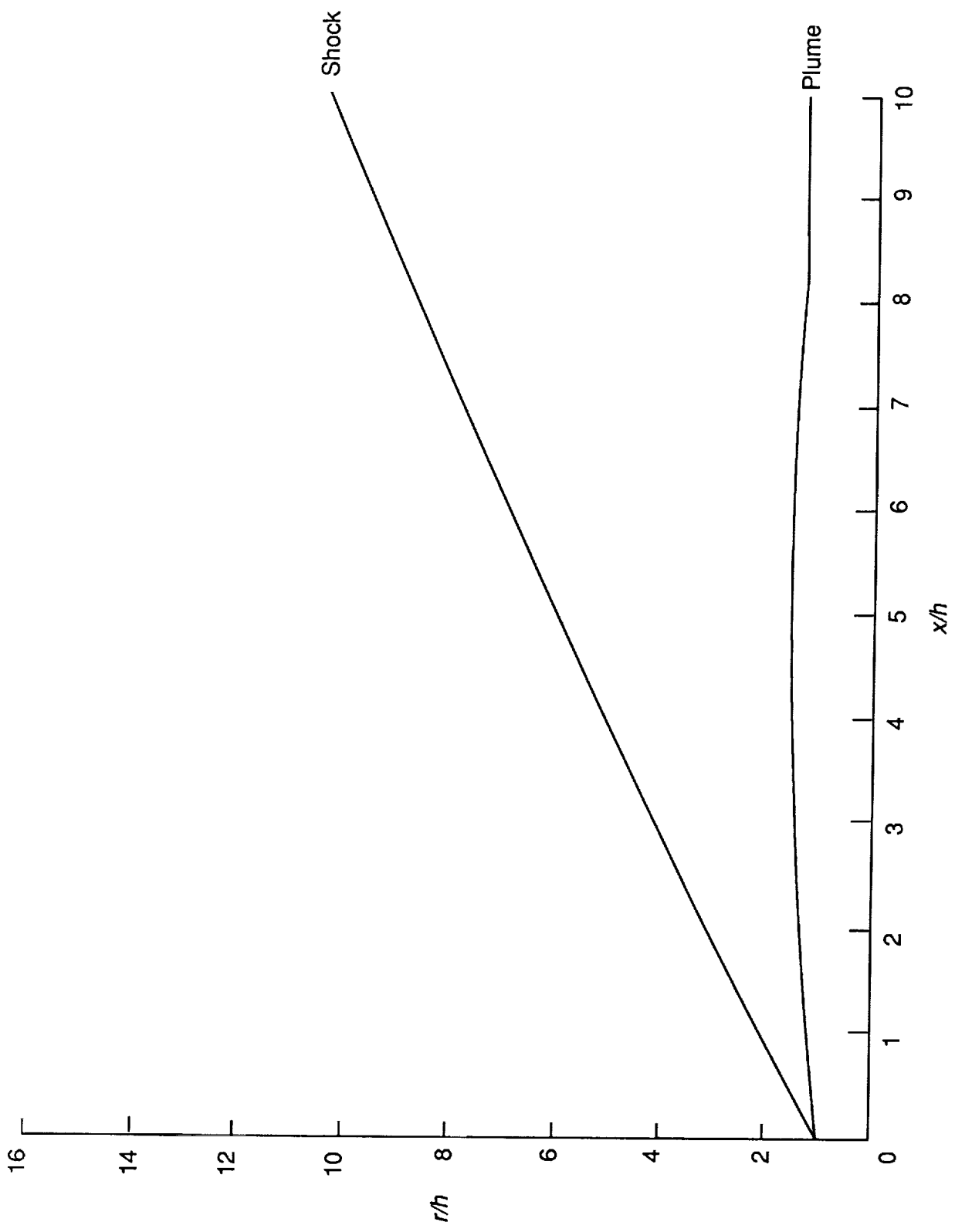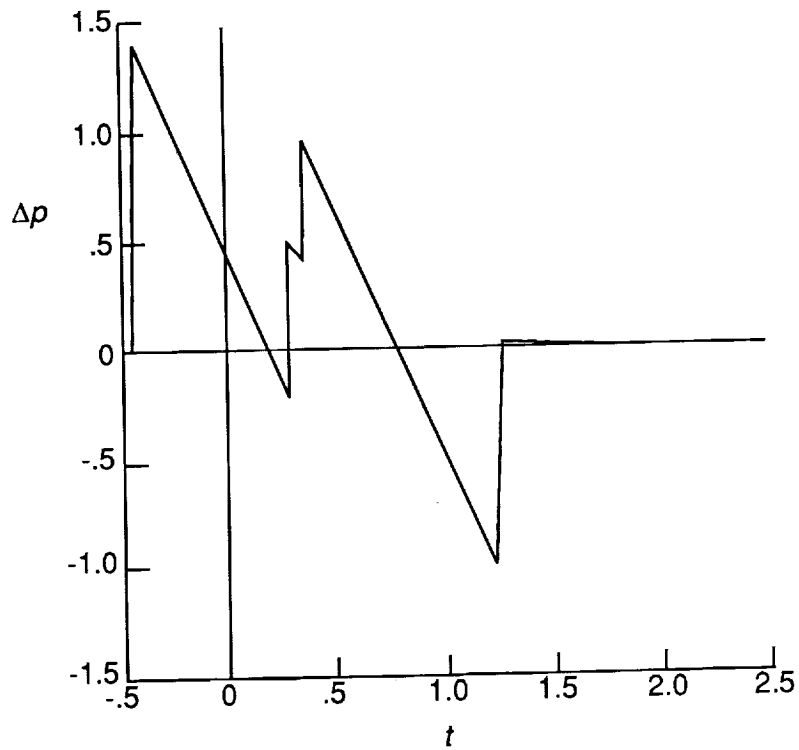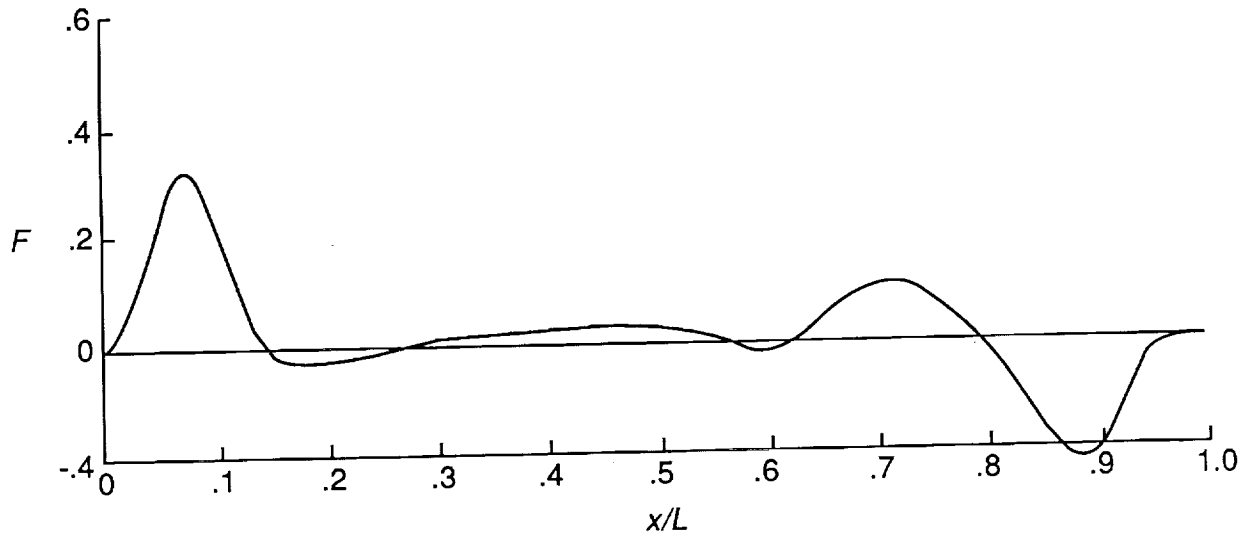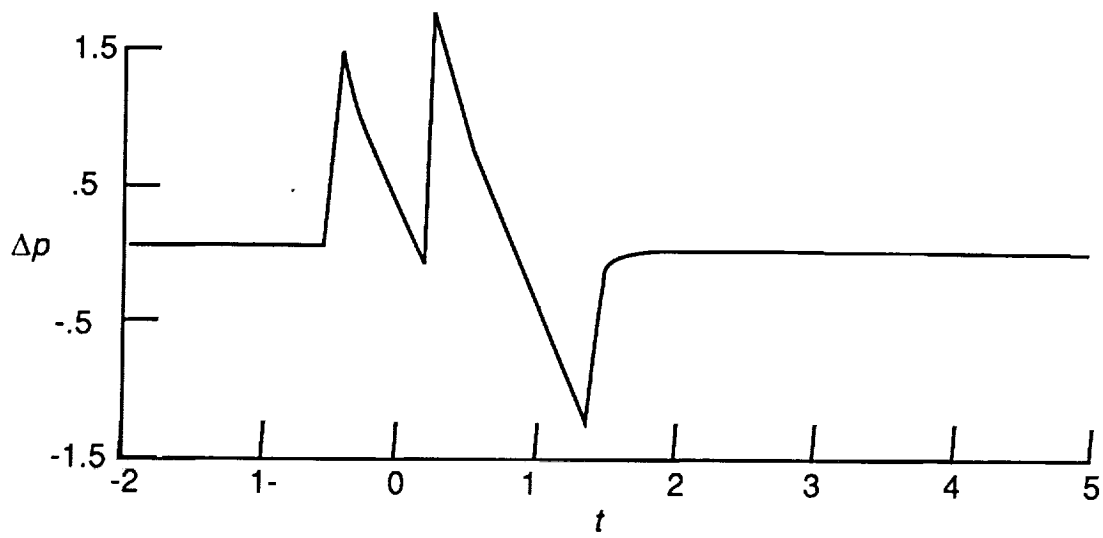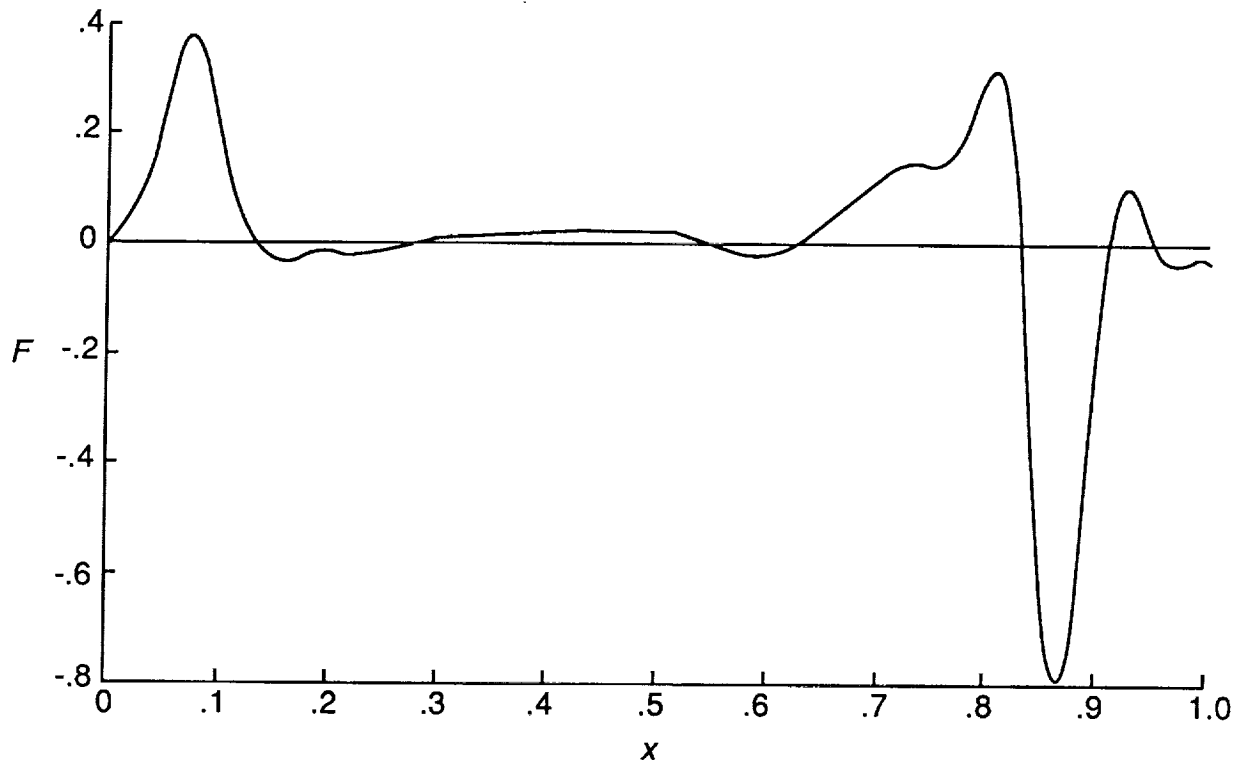
Figure 11. Computed plume shape for flight at $M_\infty = 1.6$ and altitude of $45\,000$ ft with turbo engine.

(a) Cylindrical jet.

Figure 12. F-functions and ground level signatures for low-boom configuration with cylindrical plume and computed plume of figure 11 at $M_\infty = 1.6$ and altitude of 45 000 ft with turbo engine.

(b) Computed plume of figure 11.
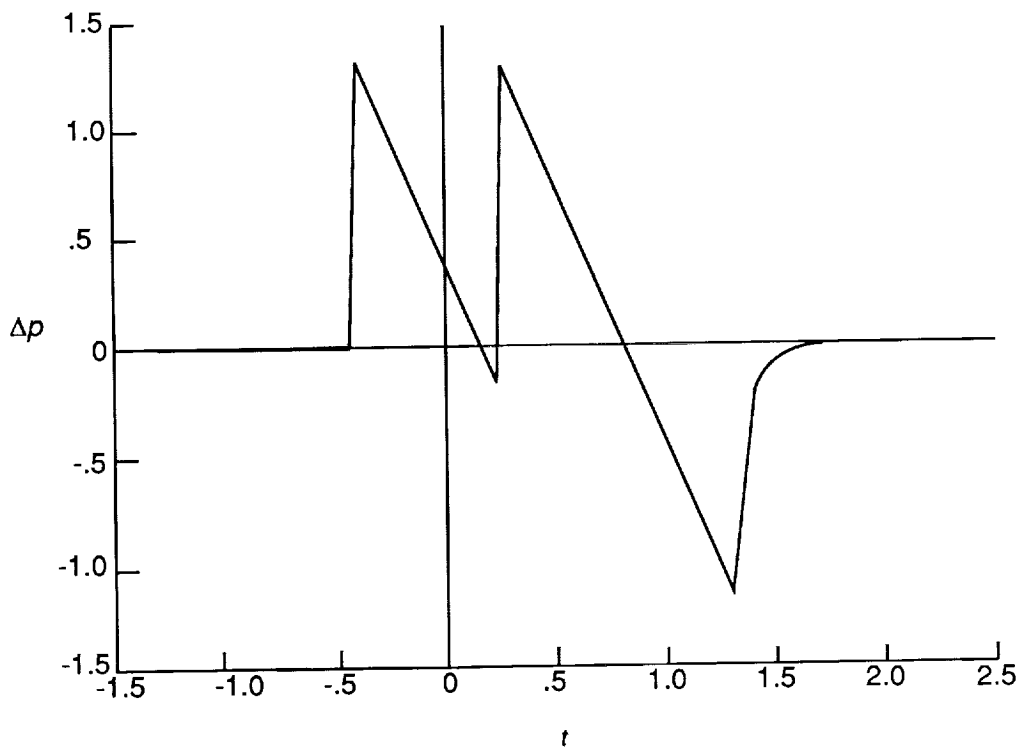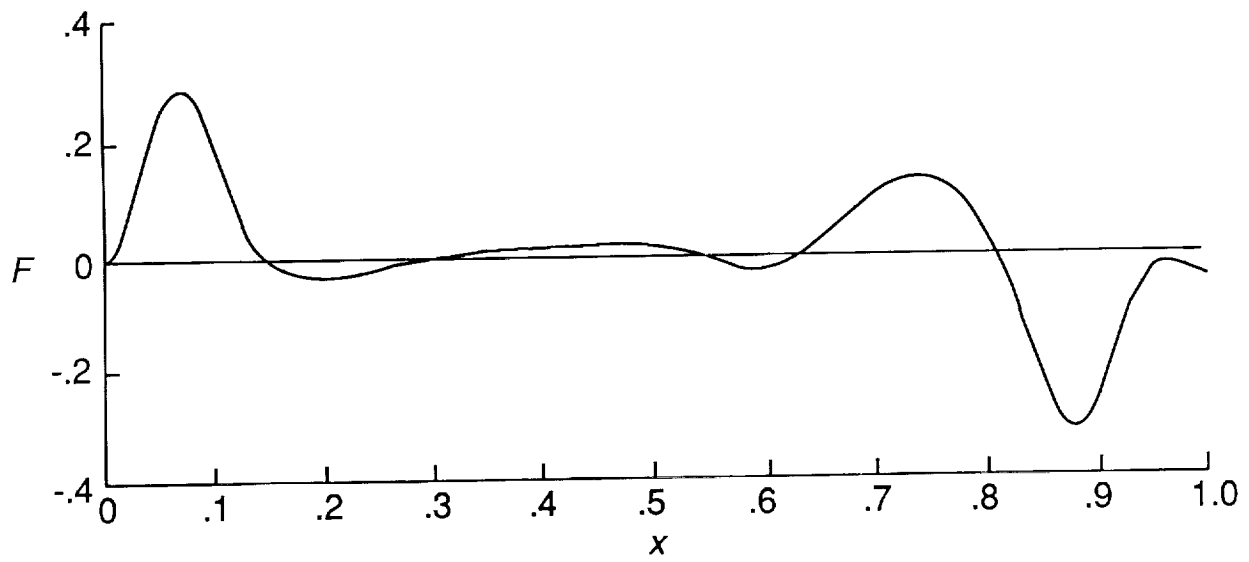
Figure 12. Concluded.

Figure 13. F-function and signature for configuration with computed plume of figure 11 at $M_\infty = 1.6$ and altitude of 45 000 ft with fuselage modified and engines staggered.
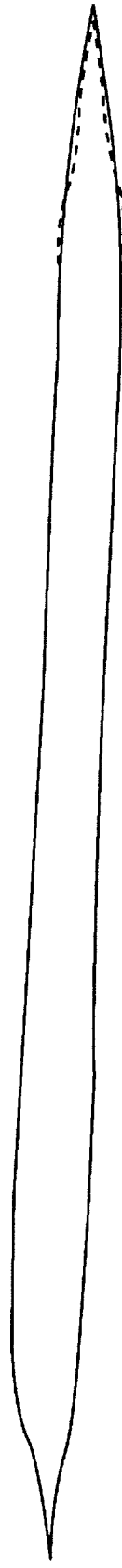
Original
Revised

Figure 14. Fuselage modification required for results of figure 13.

REPORT DOCUMENTATION PAGE

Public reporting burden for this collection of information is estimated to average 1 hour per response, including the time for reviewing instructions, searching existing data sources, gathering and maintaining the data needed, and completing and reviewing the collection of information. Send comments regarding this burden estimate or any other aspect of this collection of information, including suggestions for reducing this burden, to Washington Headquarters Services, Directorate for Information Operations and Reports, 1215 Jefferson Davis Highway, Suite 1204, Arlington, VA 22202-4302, and to the Office of Management and Budget, Paperwork Reduction Project (0704-0188), Washington, DC 20503.

1. AGENCY USE ONLY(Leave blank)	2. REPORT DATE	3. REPORT TYPE AND DATES COVERED
	March 1992	Technical Paper

4. TITLE AND SUBTITLE
Comparison of Jet Plume Shape Predictions and Plume Influence on Sonic Boom Signature

5. FUNDING NUMBERS
WU 505-59-53-01

6. AUTHOR(S)
Raymond L. Barger and N. Duane Melson

7. PERFORMING ORGANIZATION NAME(S) AND ADDRESS(ES)
NASA Langley Research Center
Hampton, VA 23665-5225

8. PERFORMING ORGANIZATION REPORT NUMBER
L-16970

9. SPONSORING/MONITORING AGENCY NAME(S) AND ADDRESS(ES)
National Aeronautics and Space Administration
Washington, DC 20546-0001

10. SPONSORING/MONITORING AGENCY REPORT NUMBER
NASA TP-3172

11. SUPPLEMENTARY NOTES

12a. DISTRIBUTION/AVAILABILITY STATEMENT

Unclassified   Unlimited

Subject Category 02

12b. DISTRIBUTION CODE

13. ABSTRACT (Maximum 200 words)
An Euler shock-fitting marching code yields good agreement with semiempirically determined plume shapes, although the agreement decreases somewhat with increasing nozzle angle and the attendant increase in the nonisentropic nature of the flow. Some calculations for a low-boom configuration with a sample engine indicated that, for flight at altitudes above 60 000 ft, the plume effect is dominant. This negates the advantages of a low-boom design. At lower altitudes, plume effects are significant but of the order that can be incorporated into the low-boom design process.

14. SUBJECT TERMS
Jet plume shape; Sonic boom; Signature

15. NUMBER OF PAGES
21

16. PRICE CODE
A03

17. SECURITY CLASSIFICATION OF REPORT	18. SECURITY CLASSIFICATION OF THIS PAGE	19. SECURITY CLASSIFICATION OF ABSTRACT	20. LIMITATION OF ABSTRACT
Unclassified	Unclassified		

NSN 7540-01-280-5500